3D Clothes Modeling from Photo Cloned Human Body

Takao Furukawa[1], Jin Gu[2], WonSook Lee[2], Nadia Magnenat-Thalmann[2]

[1] Department of Kansei Engineering, Shinshu University, Ueda, 386-8567, Japan
furukawa@ke.shinshu-u.ac.jp
[2] MIRALab, CUI, University of Geneva, Geneva, CH-1211, Switzerland
{gu,wslee,thalmann}@cui.unige.ch

Abstract. An important advantage of virtual reality technology is that real 3D objects including humans can be edited in the virtual world. In this paper, we present a technique for 3D clothes modeling based on a photo cloned human body. Photo cloning is an efficient 3D human body modeling method using a generic body model and photographs. A part segmentation technique for 3D color objects is applied for the clothes modeling, which uses multi-dimensional mixture Gaussians fitting. Firstly, we construct a 6D point set representing both the geometric and color information. Next, the mixture Gaussians are fitted to the point set by using the EM algorithm in order to determine the clusters. This approximation gives probabilities for each point. Finally the probabilities determine the segmented part models corresponding to the clothes models. An advantage of this method is that the clustering is unsupervised learning without any prior knowledge as well as integrating geometric and color data in multi-dimensional space.

1 Introduction

An advantage of digitizing information is that record, storage, playback, modification, and editing can be performed without lowering the quality. Virtual, augmented, and mixture reality techniques have recently been popularized, which is based on various technologies as well as computer vision and graphics. For example, past actors and actresses have been reproduced by computer animation[3]. However the cost for accurate human body modeling is still expensive, because it requires special equipment to measure the shape and color, and thus designers have to take long time for the modeling.

Object representation using texture mapping has become a common technique for visualizing complicated color shapes. Reasons for the recent popularity of image-based rendering techniques [15] include the recently increased availability of special hardware architecture for the texture mapping, and its application to both computer vision and graphics. A 3D human body reconstruction method using a generic body model and 2D images has been proposed[10]. This approach is simple and efficient, although it requires a special background when the pictures are taken. Photo cloning is an efficient image-based rendering technique

that generates individualized 3D human body models from photographs of people, without the need of any special equipment. Therefore we can easily immerse the virtual world by using photo cloning. The editing operation is the key area of virtual reality technology. A 3D clothes modeling technique based on the photo cloned human body enables the editing operation in the virtual world. For example, extracted clothes models can be replaced in the virtual world, and can be applied for various fields as well as e-commerce.

Our clothes modeling method is considered as a part segmentation problem in pattern recognition. Part segmentation techniques for range images have been proposed for modeling 3D parts. Proposed range image segmentation techniques can be categorized into shape- or boundary-based methods. In the boundary-based methods, segmentation has generally been performed by surface analysis based on principal curvatures, where the surface is basically assumed to be continuous. However, the principal curvatures calculated by derivatives on the surface are highly sensitive to noises, which is difficult of avoid since range images include measuring and digitizing errors. Thus, a physically-based robust boundary detection technique[21] has recently been proposed. On the other hand, shape-based methods segment the range images by fitting surfaces or volumetric primitives. Bi-quadric surface[8], supuerquadrics[8, 14] and deformation of them[17–19], and deformable surfaces[5, 4], which can be considered as 3D extension of snakes[11] were used as the primitives. Although the primitives can be deformed and combined, there are still limitations on shape representation. Furthermore, these primitive fitting methods depend on optimization techniques in which some tolerances or thresholds and appropriate initial conditions are required. Hence prior knowledge for the target objects is necessary.

Part segmentation can be basically considered as a clustering problem in statistics. In general, mixture density estimation based on function fitting is a popular way to determine clusters. Here, the central limit theorem explains the reasonable choice of Gaussian as the approximate function. The EM algorithm to estimate multi-dimensional Gaussian parameters has been applied texture image segmentation[1], motion tracking from video sequences[20], and so forth. The advantage of object description using the multi-dimensional Gaussians is that such different types of information as position, color, texture, can be integrated in the multi-dimensional space statistically.

In this paper, we present a 3D clothes modeling technique using a photo cloned human body. Here, we focus on the part segmentation technique for 3D color objects using multi-dimensional mixture Gaussians. This method does not require any primitives to describe the target objects except input geometric model. Moreover tolerances and thresholds for the fitting algorithm are not necessary. It can, therefore, be considered as learning unsupervised without prior knowledge. This paper is organized as follows: The photo cloning technique is described in section **2**, then we explain mixture Gaussian fitting and its computation in section **3**. Experimental results are presented in section **4**, and characteristics of this segmentation technique and its limitations are also discussed.

Finally we conclude this 3D clothes modeling method based on the part segmentation in section **5**.

2 Photo Cloning

Human body modeling plays important roles in various fields, for example, industrial and medical applications as well as computer graphics. Currently image-based rendering techniques have been popularized, because texture mapping gives visually real models. We have been developing a photo cloning system[13], which uses front, side, and back view photographs and generates individual 3D human body model based on a generic model. The basic concept of the photo cloning is that the lost 3D information on the photographs can be recovered by the correspondence between the photographs and the generic body model. Here we briefly describe our photo cloning technique for the human body modeling. Processes of the photo cloning are written as follows.

- Fit a generic skeleton to the front, side, and back view photographs.
- Generate an initial skin model using the correspondence between the skeleton and feature points defined on the photographs.
- Skin model modification based on the silhouette extracted from the photographs.

Fig. 1 (a) shows the generic body that consists of the skeleton and the skin surface, where contours surrounding the skeleton define the surface model. This body model is compatible with MPEG-4. The skeleton is compatible with the h-anim 1.1 specification[9], and 94 skeletal joints are used to describe the skeleton. We choose some important joints as key joints shown in fig. 1 (b). These joints give a hierarchy of skeletal parts, and define the origins of each local coordinate system in order to describe the skin parts. The basic skin model is defined by the contours, and the skin surface is deformed accordingly when the skeleton moves. Finally this skin model can be easily converted to polygonal mesh.

First, we define feature points which gives the rough silhouette on the photographs to fit the skeletal model as shown in fig. 2. Positions of these feature points are determined by interactive GUI. Here relation between the key joints and the feature points has been given, so that x-y-z coordinates of the key joints can be estimated from the feature points located in the front, side, and back view pictures. Furthermore, positions of remaining joints defined in the h-anim 1.1 skeleton are calculated by using these key joints, and then the skin contours are modified by this skeletal deformation. Consequently the fitted skeleton and contours can be generated.

Next, we describe how to make an initial skin model. Each part is represented by a polygonal mesh which has some control points. These control points are placed at certain required positions to represent the shape characteristics. Hence the skin model can be deformed by moving these control points. Furthermore, several control points are located at the boundaries between two parts, so that surface continuity is preserved when the posture of the generic body is changed.
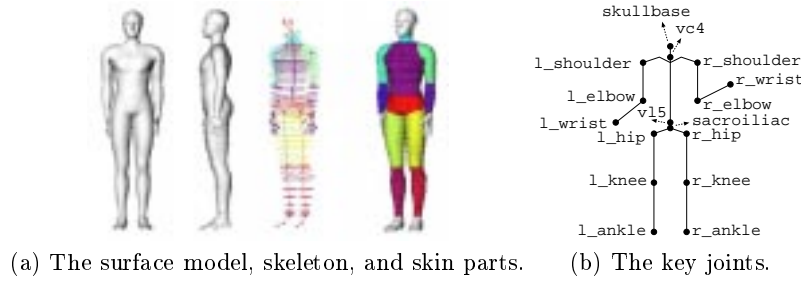
(a) The surface model, skeleton, and skin parts. (b) The key joints.

Fig. 1. The generic body model and the key joints.

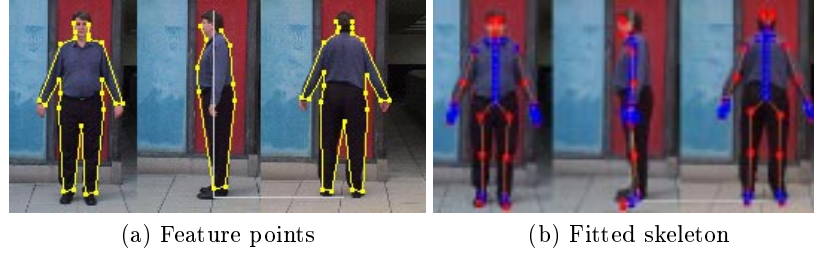(a) Feature points (b) Fitted skeleton

Fig. 2. Feature points and fitted skeleton on front, side, and back view photographs.

The accuracy of the initial skin model is insufficient, so we modify it by using the body silhouette extracted from the pictures. Here we detect the silhouette of the human body on the pictures and then fit the skin model to the silhouette. To get the silhouette, we have adopted the following algorithm.

- Apply Canny edge detector[2] for the pictures and fit line segments into edge pixels to form edge segments.
- Evaluate a connection of a pair of edge segments.
  An evaluation function for the connection E_c is defined by parameters such as angles between two segments, edge magnitudes given by Canny edge detector, and the feature points located on the pictures.
- Silhouette extraction.
  This can be considered as a path searching problem. An evaluation function E_p is defined to assess the *goodness* of a path. Here the following procedures are used.
  1. Choose an edge segment.
  2. Find a proper edge segment to connect and move to this edge segment.
  3. Repeat step 2. until the edge segment reaches the feature point, because the path terminals are given by the feature points.
  4. Assess the *goodness* of a path by calculating E_p
  5. Repeat step 1 to 4 for each edge segment and finally the best path is determined by finding the maximum of E_p.

An exact silhouette is detected by the proposed method. Finally the contours defining the skin surface are modified by using this silhouette. It can be confirmed that a visually real 3D human body model can be constructed by our method without using special equipment. Fig. 3 shows the extracted silhouette and the modified photo cloned human body.

(a) Silhouette   (b) Photo cloned body

Fig. 3. Extracted silhouette and photo cloned human body.

3   Mixture Gaussian fitting

3.1   Color coordinates and 6D vector normalization

Texture mapping gives projection from pictures to 3D geometric models, so that each pixel has geometric data as well as color data. Therefore a pixel can be represented by a 6D vector that consists of 3D geometric and 3D color components. Although a pixel is described by RGB components, it shows redundancy. Thus conversions from RGB space to YUV space have been used to reduce the redundancy[20]. Here, we use the orthogonal space defined by the principal axes, which are given by solving the eigenvalue problem of the covariance matrix of RGB components. Rotation of the basis vectors in the color space gives a geometric interpretation of this transformation.

A 6D vector is written by $(x, y, z, \xi, \eta, \zeta)$, where (x, y, z) and (ξ, η, ζ) components represent geometric and color information respectively. We determine the ξ axis by the largest eigenvalue that maximizes the variance. The η and ζ axes are determined in the order of the eigenvalues. Furthermore, we normalize geometric and color space on the condition that the maximum lengths of the bounding boxes of (x, y, z) and (ξ, η, ζ) are equal to 1. Fig. 4 shows a 6D point set obtained by the photo cloning technique, where the x, y, z axes correspond to width, height, depth, respectively. This point set is dense in x-y-z space, and so fig. 4(a) looks like geometric model. Fig. 4(b) replaces the z axis in fig. 4(a) to the ξ axis which corresponds to brightness. Fig. 4(c) plots color space where the vertical axis corresponds to the ξ. Here the number of 6D points is 119,026.
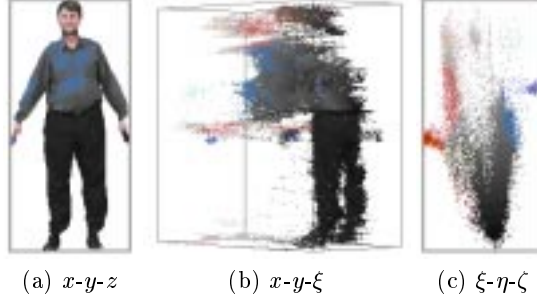
(a) x-y-z (b) x-y-ξ (c) ξ-η-ζ

Fig. 4. Projected pixels from 6D scape into 3D space.

3.2 EM algorithm

First, we denote i-th sample data in N-D space by a vector $\boldsymbol{x}_i = [\, x_{i1} \; x_{i2} \; \cdots \; x_{iN} \,]$, $(i = 1, 2, \cdots, n)$. Let the probability of $\boldsymbol{x}_i$ be $p(\boldsymbol{x}_i)$. We consider how to approximate the spatial distribution of $\boldsymbol{x}_i$ by using N-D mixture Gaussians, where the number of Gaussians is m. Next we introduce joint probability $p(\boldsymbol{x}_i, c_j)$ which is a product of the probability $p(\boldsymbol{x}_i)$ and the probability $p(c_j)$, where c_j denotes the j-th class $(j = 1, 2, \cdots, m)$. Therefore, the following relation

$$p(\boldsymbol{x}_i) = \sum_{j=1}^{m} p(\boldsymbol{x}_i, c_j) \tag{1}$$

is satisfied in discrete classes. This equation can be rewritten by using Bayes' rule

$$p(\boldsymbol{x}_i) = \sum_{j=1}^{m} p(\boldsymbol{x}_i|c_j)p(c_j), \tag{2}$$

where $p(\boldsymbol{x}_i|c_j)$ means the conditional probability of $\boldsymbol{x}_i$, given c_j. We express $p(\boldsymbol{x}_i|c_j)$ in eq.(2) by N-D Gaussian

$$p(\boldsymbol{x}_i|c_j) = \sqrt{\frac{|C_j^{-1}|}{(2\pi)^N}} \exp\left[-\frac{1}{2}(\boldsymbol{x}_i - \boldsymbol{\mu}_j)C_j^{-1}(\boldsymbol{x}_i - \boldsymbol{\mu}_j)^T\right], \tag{3}$$

where $\boldsymbol{\mu}_j$ and C_j denotes the mean vector and covariance matrix of the j-th class c_j. Moreover the coefficient of the exponential function is required for normalization of the N-D Gaussian. Furthermore, we describe each variable in eqs.(2) and (3). The mean vector of the j-th class $\boldsymbol{\mu}_j$ can be expressed by

$$\boldsymbol{\mu}_j = \sum_{i=1}^{n} \boldsymbol{x}_i p(\boldsymbol{x}_i|c_j) = \sum_{i=1}^{n} \boldsymbol{x}_i \frac{p(c_j|\boldsymbol{x}_i)}{p(c_j)} p(\boldsymbol{x}_i). \tag{4}$$

This can be rewritten by

$$\boldsymbol{\mu}_j = \frac{1}{np(c_j)} \sum_{i=1}^{n} \boldsymbol{x}_i p(c_j|\boldsymbol{x}_i). \tag{5}$$

Similarly, the covariance matrix of the j-th class can be expressed by

$$C_j = \sum_{i=1}^{n}(\boldsymbol{x}_i - \boldsymbol{\mu}_j)^T(\boldsymbol{x}_i - \boldsymbol{\mu}_j)p(\boldsymbol{x}_i|c_j) = \frac{1}{np(c_j)}\sum_{i=1}^{n}(\boldsymbol{x}_i - \boldsymbol{\mu}_j)^T(\boldsymbol{x}_i - \boldsymbol{\mu}_j)p(c_j|\boldsymbol{x}_i)$$
$$(6)$$

The expansion weights of c_j is also written by

$$p(c_j) = \sum_{i=1}^{n}p(\boldsymbol{x}_i, c_j) = \frac{1}{n}\sum_{i=1}^{n}p(c_j|\boldsymbol{x}_i). \tag{7}$$

By definition of $p(c_j|\boldsymbol{x}_i)$,

$$p(c_j|\boldsymbol{x}_i) = \frac{p(\boldsymbol{x}_i, c_j)}{p(\boldsymbol{x}_i)} = \frac{p(\boldsymbol{x}_i|c_j)p(c_j)}{\displaystyle\sum_{j=0}^{m}p(c_j)} \tag{8}$$

has been given.

An important point of the EM algorithm for mixture Gaussian fitting is that $p(\boldsymbol{x}|c_j)$, $\boldsymbol{\mu}_j$, C_j, $p(c_j)$, and $p(c_j|\boldsymbol{x}_i)$ are related to each other and a loop is formed. By setting initial values of $\boldsymbol{\mu}_j$, C_j, $p(c_j)$ and then iterating the loop, feasible mixture Gaussians can be obtained. Therefore, we can find the probability $p(c_j|\boldsymbol{x}_i)$ at which a given N-D vector $\boldsymbol{x}_i$ belongs to class c_j, and finally $\max\limits_{j} p(c_j|\boldsymbol{x}_i)$ determines the proper cluster to which $\boldsymbol{x}_i$ should belong.

3.3   Numerical calculation

The EM algorithm for multi-dimensional mixture Gaussian fitting requires that several techniques in the numerical calculation. Procedures for the numerical calculation that we have used is described as follows.

1. Set initial values.
   We initialize the mean vectors $\boldsymbol{\mu}_j$ by random numbers, and set a constant to each element of the covariance matrix C_j. Moreover, we assign $1/m$ as the initial values of the expansion weights $p(c_j)$.
2. Calculate $p(\boldsymbol{x}_i|c_j)$ by using the Gaussian written in eq.(3).
   Here, C_j^{-1} and its determinant in eq.(3) can be given by a solution of the eigenvalue problem

$$C_j\boldsymbol{s} = \lambda\boldsymbol{s}, \tag{9}$$

   where λ and $\boldsymbol{s}$ denote the eigenvalue and the eigenvector. If we determine λ and $\boldsymbol{s}$ on the condition that $\boldsymbol{s}$ gives normalized orthogonal bases, i.e. $\boldsymbol{s}_k \cdot \boldsymbol{s}_l = \delta_{kl}$,

$$C_jS = S\Lambda \tag{10}$$

is given. Here

$$
\Lambda = \begin{bmatrix} \lambda_1 & & & 0 \\ & \lambda_2 & & \\ & & \ddots & \\ 0 & & & \lambda_m \end{bmatrix}, \ S = \begin{bmatrix} s_1 \ s_2 \cdots s_m \end{bmatrix}.
\tag{11}
$$

By using eq. (10), the inverse matrix of C_j can be expressed by

$$
C_j^{-1} = S\Lambda^{-1}S^T.
\tag{12}
$$

Of course the diagonal elements of Λ^{-1} are $1/\lambda_k$. Furthermore, $|C_j^{-1}|$ in the coefficient of the exponential function can be replaced by the trace

$$
|C_j^{-1}| = \prod_{k=1}^{N} 1/\lambda_k.
\tag{13}
$$

Therefore we can find $p(\boldsymbol{x}_i|c_j)$.
3. Calculate $p(\boldsymbol{x}_i)$ by using eq. (2).
   $p(c_j)$ and $p(\boldsymbol{x}_i|c_j)$ have already been given in step 1 and 2.
4. Assign $p(\boldsymbol{x}_i|c_j)$ and $p(c_j)$ into eq. (8) and get $p(c_j|\boldsymbol{x}_i)$.
5. Rewrite each mean vector $\boldsymbol{\mu}_j$ and covariance matrix C_j by using eqs. (5) and (6), and then return to step 2. and repeat these procedures.

We have used `dspev` in LAPACK[12] to solve eigenvalue problem, since the covariance matrix C_j is a positive symmetry matrix. When a small value is assigned into the initial covariances, $|C_j^{-1}|$ in eq. (3) calculated by eq. (13) may overflows. Thus large covariances are feasible for the initial values.

3.4 Geometric model for segmented object

Although the pixel distribution in x-y-z space represented by 6D vectors are used for clustering, we need to construct a geometric model of segmented objects finally. Geometric objects to be segmented have been represented by triangular faces, and each face contains the corresponding pixels. Furthermore, the probability $p(c_j|\boldsymbol{x}_i)$ for each pixel has been calculated, so we simply define the probability of c_j given triangular face y_k by using the average

$$
p(c_j|y_k) = \frac{1}{K} \sum_{\boldsymbol{x}_i \in y_k} p(c_j|\boldsymbol{x}_i),
\tag{14}
$$

where K is the number of pixels contained in the triangular face y_k.

4   Experimental results

Fig. 5 shows the result of a 6D mixture Gaussian fitting where four Gaussians are used. Standard deviation of 6D Gaussians are drawn by color ellipses in fig. 5(a)-(d), where longitude and latitude lines of 6D ellipsoids defined by the standard deviation are projected into 3D space. Here, the initial mean vectors are given by random variables as shown in fig. 5 (a) and (b). All initial standard deviations are 0.1. Converged Gaussians are illustrated in fig. 5 (c) and (d), where the number of iterations is 128. Although initial Gaussians do not fit the input data, experiments show the proper convergence can be reached by the EM algorithm. Yellow and red ellipsoids in x-y-z space illustrated fig. 5 (c) show that the blue shirt part and the black trouser form each cluster. On the other hand, fig. 5 (d) shows that blue, black, and mainly skin color clusters are formed, where these clusters are illustrated by red, yellow, and green ellipsoids respectively.
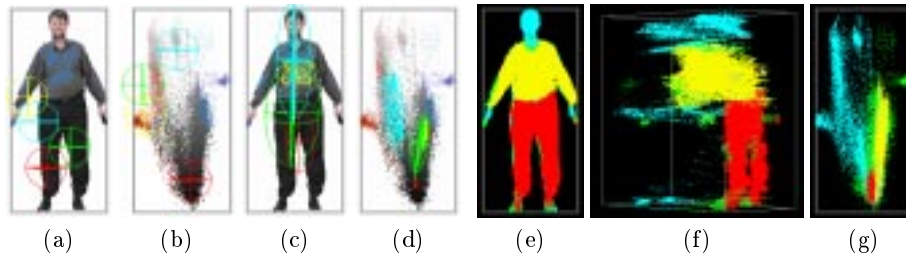

(a)   (b)   (c)   (d)   (e)   (f)   (g)

Fig. 5. A 6D mixture Gaussian fitting by using the EM algorithm where four Gaussian are used. Initial conditions for the EM algorithm in x-y-z and color space are illustrated in (a) and (b), and the converged result is illustrated in (c) and (d). Colored pixels in (e)-(g) show the clustered result where coordinates systems are x-y-z, x-y-ξ, and ξ-η-ζ.

Fig. 5 (e)-(g) show the clustered pixels in x-y-z, z-y-ξ, and ξ-η-ζ spaces. Each pixel has $p(c_j|\boldsymbol{x}_i)$, which is the probability of c_j given $\boldsymbol{x}_i$, so that the $\max_j p(c_j|\boldsymbol{x}_i)$ determines a class to which the pixel $\boldsymbol{x}_i$ should belong. Since the pixels corresponding to the black trouser form the dense cluster in the color space and distribute in the lower part on the y axis, this part is detected exactly. The blue shirt is extracted approximately, however it is not exact at the boundary part. Skin color face and hands are also detected, and this cluster distributes large areas in both the spatial and color space. Thus the accuracy is insufficient.

Fig. 6 shows the convergence process of the EM algorithm, where the color ellipsoids illustrate 6D Gaussinans. Fig. 6(a) and (b) are plots of x-y-z and ξ-η-ζ spaces respectively. Here the iteration steps are 1, 4, 8, and 32, and the initial condition and the convergence have been shown in fig. 5(a)-(d). Although Gaussians are distributed randomly at the beginning, the first EM step brings them close to the mean vector of the entire data. The standard deviations are
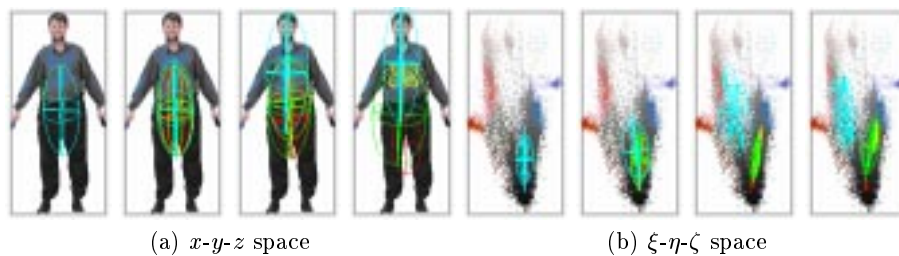
(a) x-y-z space　　　　　　　　(b) ξ-η-ζ space

Fig. 6. Convergence process of the EM algorithm, where the numbers of iterations are 1, 4, 8, and 32 respectively.

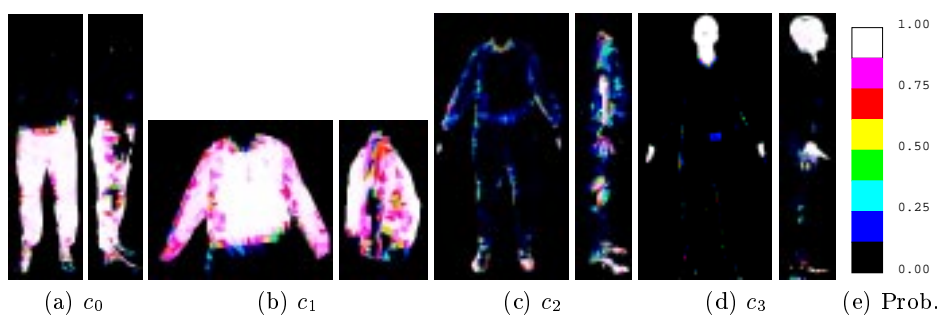(a) c_0　　　　(b) c_1　　　　(c) c_2　　　　(d) c_3　　(e) Prob.

Fig. 7. Probability distributions on the human body model, where the probability interval $[0, 1]$ corresponds to the color sequence shown in (e).
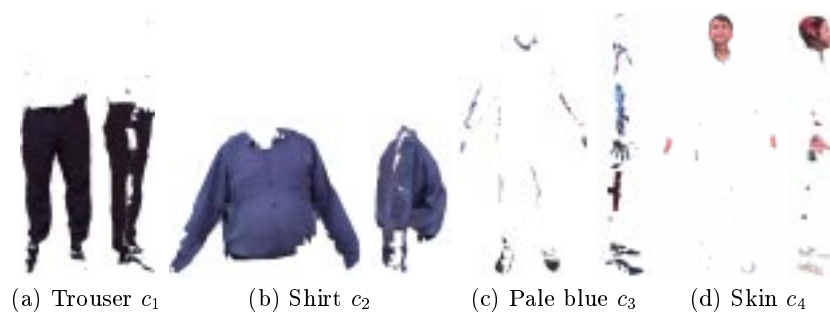

(a) Trouser c_1　　　(b) Shirt c_2　　　(c) Pale blue c_3　　(d) Skin c_4

Fig. 8. Extracted parts given by the highest probability of each triangular face.

also similar. Thus, the red, yellow, and green ellipsoids are covered by cyan ellipsoids in fig. 6(a). These Gaussians then start to make clusters in further iterations of the EM, and finally reach convergence. In this case, the result of the 32th iteration shown in fig. 6 gives the convergence approximately.

Probability distributions $p(c_j|y_k)$ defined on the photo cloned human body surfaces are shown in fig. 7, where the probability are shown by the color bar in fig. 7 (e). Fig. 7(a),(b),(d) show that the probabilities at the black trouser, blue shirt, head and hand parts are close to 1. On the other hand, the probabilities at side parts appearing in fig. 7(c) are not very high. Therefore, the reliabilty of the formed cluster c_3 is relatively low.

Fig. 8 shows the segmented 3D color parts represented by the triangular faces with textures. The whole human body is segmented to the black trouser, blue shirt, pale blue part and mainly skin color part. These geometric parts are determined by the highest probability of the triangular faces. Side parts shown in fig. 8(c) should be discriminated as the trouser and shirt, though these parts are independent. This is caused by inaccuracy of the input data, so that it will be difficult to correct them without the prior knowledge for the target object.

5   Conclusions

We have proposed 3D clothes modeling technique based on a photo cloned human body. The human body model can easily be generated by using the photo cloning technique without any special equipment. In this paper, we focused on a part segmentation technique for 3D color object based on multi-dimensional mixture Gaussians using the EM algorithm. An advantage of the proposed method is that geometric and color data can be integrated in multi-dimensional space, insufficient geometric information to be compensated by color data, which allows the face and hand of the test object are recognized as a single part, even though they are isolated spatially. Furthermore, the clustering can be performed by unsupervised learning without any tolerances or thresholds used for the Gaussian fitting. The convergence process of the EM algorithm is also observed. We could construct the segmented geometric models represented by triangular faces. Consequently 3D clothes models are extracted from the photo cloned human body. However, there are several problems to be solved as well as the accuracy, for example how many Gaussians are required for feasible segmentation and its evaluation still remains. these are problems to be solved.

6   Acknowledgements

References

1. Belongie, S., Carson, C., Greenspan, H., and Malik, J." "Color- and Texture-Based Image Segmentation Using EM and Its Application to Content-Based Image Retrieval," Proc. ICCV98 (1998) 675-682
2. Canny, J., A Computational Approach to Edge Detection, IEEE Trans. PAMI, **8** (1986) 679–698
3. Carignan, M., Yang, Y., Thalmann, N. M., and Thalmann, D., Dressing Animated Synthetic Actors with Complex Deefromable Clothes, Proc. SIGGRAPH '92 (1992) 99–104
4. Caselles, V., Kimmel, R., Sapiro, G., Sbert, C, Minimal-Surfaces Based Object Segmentation, IEEE Trans. PAMI, **19** (1997) 394–398
5. Cohen, I., Cohen, L. D., and Ayache, N., Using Deformable Surface to Segment 3-D Images and Infer Differential Structures, CVGIP Image Understanding, **56** (1992) 242–263
6. Gershenfeld N., The Nature of Mathematical Modeling, Cambridge University Press (1999)
7. Gu, J., Chang, T., Gopalsamy, S., and Shen, H., A 3D Reconstruction System for Human Body, Proc. CAPTECH'98, (1998) 229–241
8. Gupta, A., and Bajcsy, R., Volumetric Segmentation of Range Images of 3D Objects Using Superquadric Models, CVGIP Image Understanding, **58** (1993) 302–326
9. VRML Humanoid Animation Working Group: The VRML Humanoid Specification Version 1.1 `http://ece.uwaterloo.ca/~h-anim/spec1.1/`
10. Hilton, D. B., Gentils T., Smith, R., and Sun, W., Virtual People: Capturing Human Models to Populate Virtual Worlds, Proc. of Computer Animation '99 (1999) 174–185
11. Kass, M., Witkin, A., and Terzopoulos, D., Snakes: Active Contour Models, International Journal of Computer Vision, **1** (1998) 321–331
12. Anderson, E, *et al.*, LAPACK Users' Guide 3rd Ed., Society for Industrial and Applied Mathematics, Philadelphia, PA (1999)
13. Lee, W., Gu, J., Magnenat-Thanlmann, N., Generating Animatable 3D Virtual Human from Photographs, Proc. Eurographics 2000 (to appear)
14. Leonardis, A., Jaklie A., and Solina, F., Superquadrics for Segmenting and Modeling Range Data, IEEE Trans. PAMI, **19** (1997) 1289–1295
15. McMillan, L. and Gortler, S, Image-Based Rendering: A New Interface Between Computer VIsion and Computer Graphics, Computer Graphics, **33**, No. 4, (1999) 61–64
16. Moghaddam, B., Nastar, C., and Pentland, A., A Bayesian Similarity Measure for Direct Image Matching, Proc. ICPR'96 (1996) B7E.5
17. Pentland, A. P., Automatic Extruaction of Deformable Part Models, Internaltinal Jounral of Computer Vision, **4** (1990) 107–126
18. Pentland, A. P., and Schlaroff, S., Closed-Form Solution for Phisycally Based Shape Modeling and Recognition, IEEE Trans. PAMI, **13** (1991) 715–729
19. Terzopoulos, D., and Metaxas, D., Dynamic 3D Models with Local and Global Deformations: Deformable Superquadrics, IEEE Trans. PAMI, **13** (1991) 703–714
20. Wren, C., Azarbayejani, A., Darrell, T., and Pentland, A., Pfinder: Real-Time Tracking of the Human Body, IEEE Trans. PAMI, **19** (1997) 780–785
21. Wu, K., Levine, M. D., 3D Part Segmentation Using Simulated Electrical Charge Distribution, IEEE Trans. PAMI, **19** (1997) 1223–1235